24th COBEM - 2017

24th ABCM International Congress of Mechanical Engineering
December 3-8, 2017, Curitiba, PR, Brazil

COBEM-2017-2666
USE OF FINITE ELEMENT METHOD TO VALIDATE THE TEMPERATURE FIELD OF A 5-AXIS MACHINING CENTER

Marcelo Otávio dos Santos
School of Engineering of the University of Sao Paulo – Dept. of Mechatronics and Mechanical Systems Engineering - Laboratory of Manufacturing Engineering - Av. Prof. Mello Moraes, 2231, Cidade Universitária, 05508-900, Sao Paulo, SP, Brazil.
Instituto Mauá de Tecnologia (IMT) - Centro Universitário Mauá – Campus- São Caetano do Sul - Praça Mauá 1 - 09580 900 - São Caetano do Sul – SP - Brazil.
FEI – Centro Universitário Padre Saboia de Medeiros – Av. Humberto de Alencar Castelo Branco, 3972, Bairro Assunção, 09850-901, S. Bernardo do Campo, SP, Brazil.
marcelootavio@usp.br , marcelo.santos@maua.br , *mosantos@fei.edu.br*

Éd Claudio Bordinassi
Instituto Mauá de Tecnologia (IMT) - Centro Universitário Mauá – Campus- São Caetano do Sul - Praça Mauá 1 - 09580 900 - São Caetano do Sul – SP - Brazil.
ecb@maua.br

Gilmar Ferreira Batalha
School of Engineering of the University of Sao Paulo – Dept. of Mechatronics and Mechanical Systems Engineering - Laboratory of Manufacturing Engineering - Av. Prof. Mello Moraes, 2231, Cidade Universitária, 05508-900, Sao Paulo, SP, Brazil.
gilmar.epusp@gmail.com

Abstract. *In current manufacturing processes, 5-axis machining centers play an important role machining parts with complex geometry and that require high dimensional accuracy. This research aims to develop an efficient method to simulate the thermal-structural performance of a 5-axis machining center, through the study of their main subassemblies such as ball screw system, linear guides and spindle under real load conditions. The methodology was based on an experimental survey of the machine's thermal behavior using temperature sensors and thermal imaging, with simultaneously numerical validation using the Finite Elements Method (FEM), under adequate boundary conditions. The temperature gradient at predetermined periods could be obtained by FEM, through an interface model that includes frictional contact, heat exchange in the contact area, frictional heating and convective heat exchange. The results of the simulations show that the methodology is an effective tool to determine the thermal field of the machine correlating the reading of temperatures at strategic points obtaining a maximum error of less than 9.6%. The conclusion is that the method, when appropriate boundary conditions are considered, is a proper feature for simulating the machine thermal behavior, which can still be used in the design phases of the equipment.*

Keywords: *5-axis machining center, finite element method, thermal field measurement, thermal field simulation, friction heat generation.*

1. INTRODUCTION

Errors in manufacturing processes should be minimized to supply products with high precision and proper quality. These errors include geometric errors of machine components, thermal errors induced by temperature variations, deflection errors caused by cutting forces, servo errors of the machine axis, NC interpolation algorithmic errors, and others (Lee *et al*., 2003). Among those, thermal errors account for 40-70% of the total errors (Ramesh *et al*., 2000). In this scenario, numerical methods have been proved to be powerful tools to simulate heat transfer and thermoelastic behavior of machine tools, in which temperature fields and thermal deformations are difficult to measure due to the high complexity of the machine tool structure (Zwingenberger *et al*., 2008). Numerical models validated through experimental results may reduce the time and cost associated with multiple experiments (Liu et al., (2017).

The finite element method (FEM) allowed an in-depth analysis of the machine tools' thermal behavior under the influence of heat sources present both inside and outside the machine structure. Additionally, the effect of the structural components individually could be examined by FEM, both those incorporating the heat sources, as well as those subject

to the influence of external heat sources, i.e. by varying the ambient temperature (Großmann, K., 2015). Finite element formulations for the frictional contact and frictional heating based on classical Coulomb-type friction have been discussed in Wriggers and Miehe (1994). Xu et al., (2011) established the thermal deformation FEM model of the ball screw of a machine tool to predict and to compensate the thermal error caused by the frictional heating. Xu et al. (2007) studied the influences of the bearing temperature on the heat transfer of machine tools and improved the accuracy of the FEM thermal error model. In 2007, Zhao et al. established the thermal deformation of the spindle to predict and to compensate the thermal error caused by the spindle heating during operation. Zwingenberger, *et al*., (2008) experimentally monitored the temperature fields of a 4-axis machining center using temperature sensors located at strategic points in the machine. The known temperature results allowed to numerically simulate the machine behavior by the finite element method. Großmann *et al*., (2013) presented a thermal efficiency simulation technique for a vertical machining center under various rotational speeds using FEM. The temperature field distribution, the mechanism and the shape of the thermal deformation were analyzed. The simulation of the thermal deformation of the machine presented characteristics consistent with the results experimentally obtained. Souza (2013) used the finite element model of a 3-axis machine tool to virtually evaluate the efficiency of a ball bar system to predict thermal displacements. Xu and Li (2017) analyzed the thermal coupling of a ball screw system with internal cooling of a boring-milling machining center through finite element modeling. The thermal boundary conditions were obtained through empirical relations. Thermo-elastic models that can be simulated for the overall system consisting of machine tool, process and environment are required designing compensation solutions, the evaluation of thermo-elastic behavior and the correction of thermoelastic errors during machine tool operation (Feng et al., 2015).

This research aims at developing an efficient method to simulate the thermal-structural performance of a machining center and their subassemblies under real load conditions. This method can be an important tool to evaluate the thermal-structural behavior still in the design development phases, complemented by the calculation algorithm, the modeling, simulation and evaluation process that can be completely executed at the FEM system level. For calculating the thermal-structural system behavior, ANSYS provided several coupled-field elements (such as SOLID226). This enabled strong coupling of the thermal and structural engineering field problems to model the heat transfer occurring on the contact surface. First, to analyze the thermal-structural problem, the exclusive thermal field was calculated in process, including kinematics.

2. EXPERIMENTAL PROCEDURE

The machine studied was a 5-axis horizontal machining center installed in an environment with ± 2 °C controlled room temperature (Fig. 1). The objective of the experimental stage was to take the complete thermal profile of the machine under different working conditions, using temperature sensors and thermal imaging. Next, a model of the machine and its subsystems was developed using the finite element method with validation for all the analyses experimentally performed.

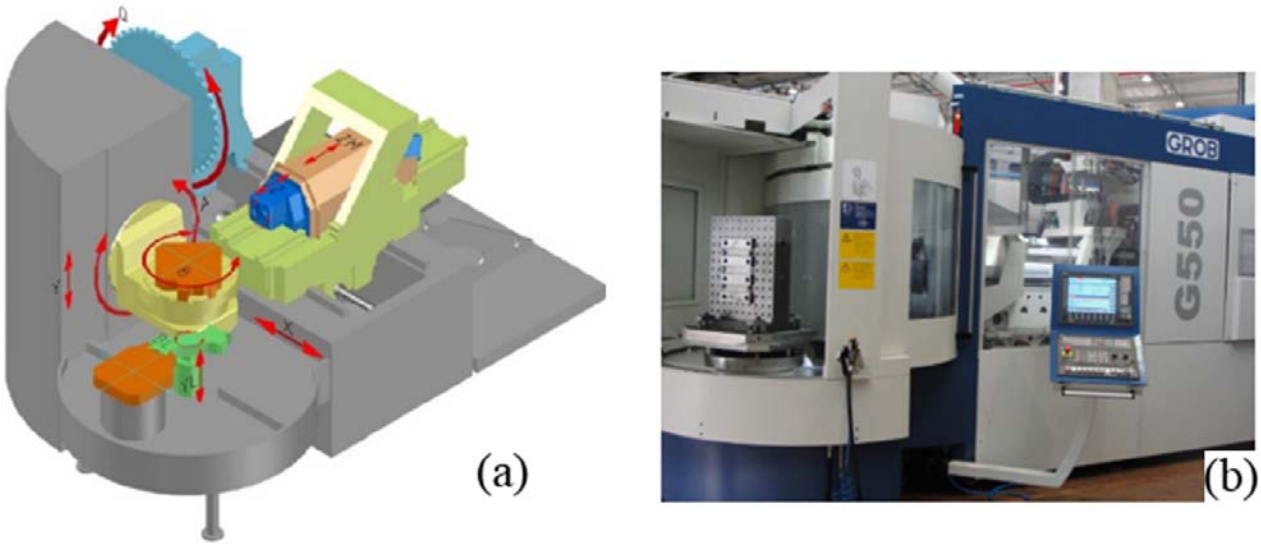

Figure 1. (a) Schematic of the machining center kinematics studied, (b) photo of the machining center installed in the technological application center - TAC.

For surveying experimental data which served as a reference for validating the model in finite element of the machine, three testing stages were carried out. In the first stage, only the X-axis slide unit was moved at a speed of 30 m per minute for 6 hours. At this stage, the thermal behavior of the ball screw nut and the linear guide rail were evaluated. At the second stage, only the spindle was moved with a rotational speed of 16,000 rpm, whereby it was possible to evaluate the thermal behavior of the spindle tip for 6 hours. At the third stage, the three linear axes X-Y-Z and the driver spindle were moved at speed of 30 m/min. and 10,000 rpm respectively, for a total period of 4 hours, which allowed evaluating the thermal behavior of the complete machine. A 14-hour interval was taken between each cycle, by stopping the machine to return it to room temperature. The strokes and speeds tested are shown in Table 1.

Table 1. Experimental conditions

X-axis speed	**Y-axis speed**	**Z-axis speed**	**Spindle rotational speed**
30 m/min	30 m/min	30 m/min	16,000 rpm ; 10,000 rpm
X-axis stroke	**Y-axis stroke**	**Z-axis stroke**	**----**
800 mm	950 mm	1020 mm	

Fifteen temperature sensors were installed and distributed at strategic points in the machine structure. Figure 2 illustrates the exact placement of the fifteen installation points of the sensors. Sensor T14 was submerged in the coolant tank of the machine to monitor the thermal behavior of the coolant passing through the base of the machine. The room temperature monitoring sensor T15 was installed outside the machine to avoid any influence. An infrared camera was also used to monitor the temperature at difficult access points. Fig. 3 shows the temperature sensor T2 installed on the X-axis ball screw motor bearing flange (a) and its thermal imaging (b).

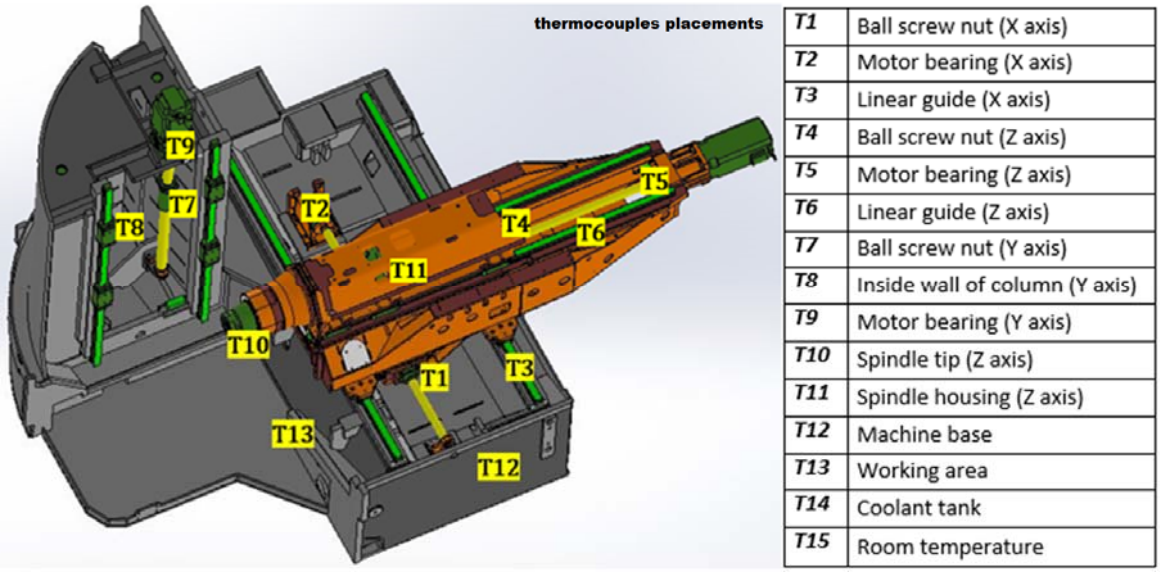

T1	Ball screw nut (X axis)
T2	Motor bearing (X axis)
T3	Linear guide (X axis)
T4	Ball screw nut (Z axis)
T5	Motor bearing (Z axis)
T6	Linear guide (Z axis)
T7	Ball screw nut (Y axis)
T8	Inside wall of column (Y axis)
T9	Motor bearing (Y axis)
T10	Spindle tip (Z axis)
T11	Spindle housing (Z axis)
T12	Machine base
T13	Working area
T14	Coolant tank
T15	Room temperature

Figure 2. Installation placement points of the fifteen thermocouples in the machine tool.

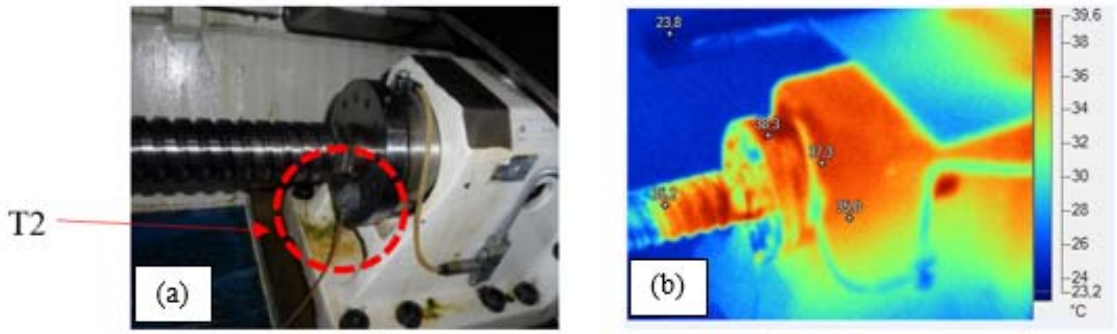

Figure 3. (a) T2 - thermocouple installed on the X-axis ball screw rear bearing, (b) and its thermal image.

The subsystems analyzed in this research were the linear guide and ball screw from the X axis (a) and the spindle (b), as indicated in Fig. 4.

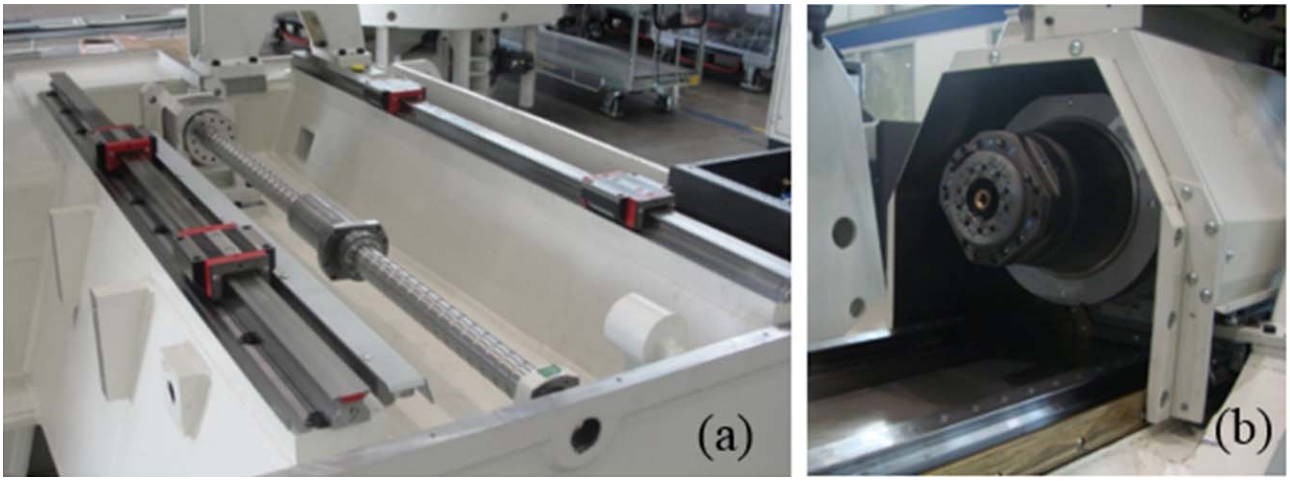

Figure 4. (a) X-axis ball screw and linear guide system, (b) spindle.

3. NUMERICAL PROCEDURE

ANSYS Workbench (WB) and Classic ANSYS Parametric Design Language (APDL) were used to model and to validate the transient thermal behavior of the machining center. For the purposes of this work, the use of the finite element method (FEM) as an important method of predicting thermal errors is based on the following simplifying assumptions:

- The grooves in the ball screw axis were disregarded; hence, the axis is a solid cylinder.
- The friction coefficient between the nut and the ball screw shaft, as well as between the bearings and the shaft, have constant value according to the manufacturer's specifications.
- Heat generation due to frictional dissipation.
- Frictional dissipated energy generates the heat to both the contact and target surfaces.
- The convective coefficient was previously calculated in ANSYS CFX, considering the forced convection during the axis movement.

The general considerations for the analyses were as follows:

- Base material: Steel St37-2 – DIN 17100.
- Ball screws shaft and linear guide rail material: Carbon steel AISI 52100 – DIN 17230.
- Slide units housing material: Ductile cast iron GGG-60 – DIN 1693-1/2.
- Total analysis interval: 0 to 21,600 s.
- The thermal mapping of the machine was considered every 360s.
- Thermal boundary conditions (BC): Heat generation by friction between the machine sliding elements.

To implement the modeling of heat generation due to friction, the functions available in ANSYS were combined, i.e. Workbench and Classic. This methodology is useful since it is possible to approach the structure of the existing problem more heuristically in ANSYS-Workbench, which is similar to a CAD program. Subsequent processing in ANSYS-Classic is necessary for the coupled transient thermal-structural analysis; however, it simultaneously enables the execution of exact and reproducible simulations due to the implementation and application of APDL scripts. The investigations aimed at integrating the physical interaction of stationary and moving assemblies into simulation. Since defined translational kinematic profiles were mapped, the model structure was known at all points during the analysis, so that the heat flow caused by friction could be manually applied as the Coulomb-type boundary condition to the contact zone. Also, the model structure was identified through the ANSYS element technology oriented to contact mechanics (such as CONTA174 and TARGET170), which later defined the heat flow exchanged by conduction through the temperature conditions shown in the contact zone. For the three subsystems analyzed in this research, such as ball screw, linear guide and spindle, three CAD models were developed to represent the geometries of the parts in contact according to the actual design of the respective components. Figure 5 shows the scheme of the contacts created in the ANSYS for friction generation, being (a) contact between the rail and the carriage of the linear guide, (b) contact between the nut and the ball screw shaft, and (c) contact between the bearings and the motor inside the spindle.

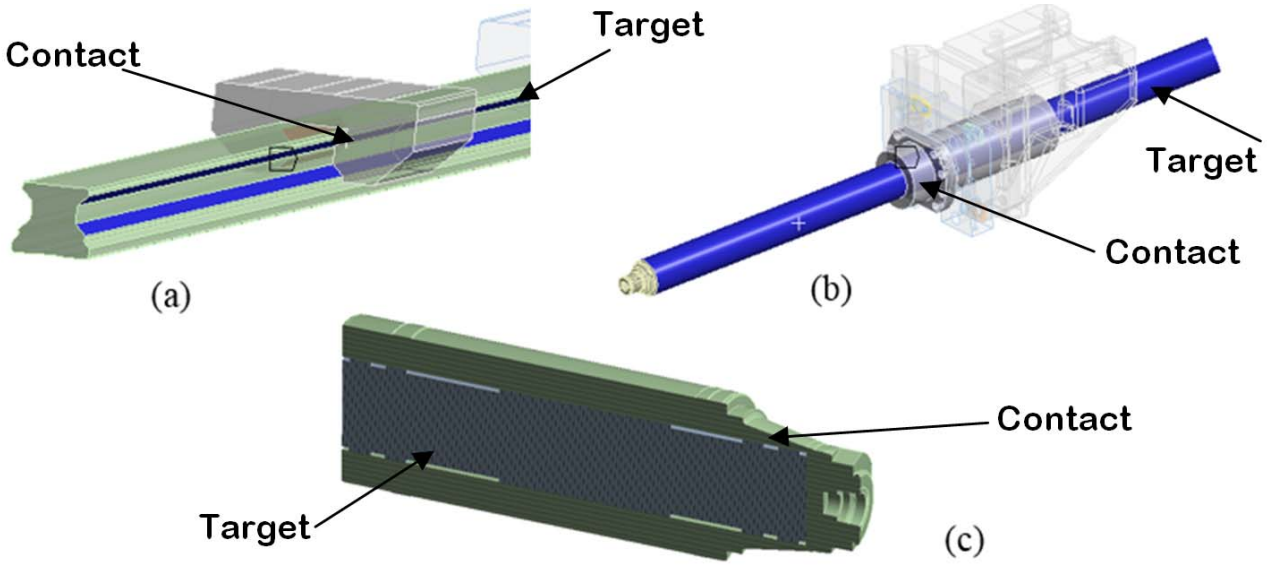

Figure 5. Schematic of the thermal contacts created in the ANSYS for the frictional heat generation. (a) linear guide, (b) ball screw, (c) spindle.

Figure 6 shows the finite element mesh created for the linear guide, ball screw and spindle. The mesh control was mainly conducted through meshing the basic area and had to be performed according to the physical requirements of the system to be simulated. In this case, a very fine meshing of the thermally active contact regions was produced. The Coupled-Field elements required for the motion are currently only available in ANSYS Classic, therefore requiring an APDL script to implement it in ANSYS Workbench.

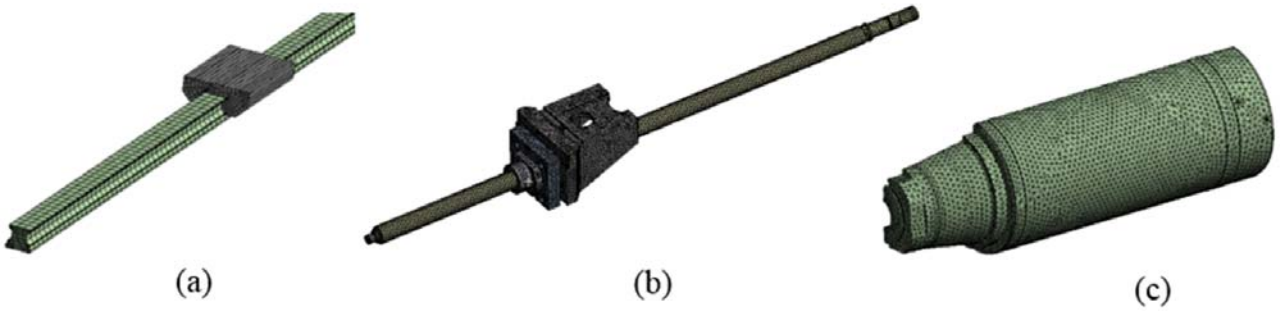

Figure 6. Finite element mesh generated for subsystems (a) linear guide, (b) ball screw, (c) spindle.

The type of element used in the linear guide meshing was the 20-node hexahedron with element size of 20 mm in the rail, and 10 mm in the carriage. At an X-axis slide unit speed of 30 m/min., the heat rate at the contact between the carriage and the rail reached 18 W, with a friction coefficient, $\mu = 0.35$. The convective heat transfer coefficient at the rail surface was 20 W/m^{2}K.

For the ball screw system, at an X-axis slide unit speed of 30 m/min., the heat generated at the contact of the nut with the shaft reached 48 W with friction coefficient equaled to 0.38. The heat rate in the front bearing reached 12 W, while the heat rate in the rear bearing reached 17 W. The convective heat transfer coefficient between the shaft surface and the ambient was 42 W/m^{2}K, and at the nut surface was 34 W/m^{2}K. The corresponding finite element meshing was composed of a 10-node tetrahedral element type, and a 10-mm element in the shaft, and 15-mm in the nut.

For the spindle model, the heat generated in the rear bearing equaled 147 W, the heat generated in the front bearing equaled 93 W and the heat generated in the motor equaled 342 W, with a spindle rotational speed of 16,000 rpm, considering the surrounding air. The front bearing displayed a restriction to the axial displacement to decrease the effect of the spindle tip expansion, whereas the rear bearing moved freely in the axial direction. The forced convection heat transfer coefficient on the outer surface of the calculated spindle tip was 58 W/m^{2}K. The spindle finite element meshing consisting of a 10-node tetrahedral mesh with 20-mm elements was used.

4. RESULTS AND DISCUSSION

Figure 7 graph demonstrates the measurement and simulation results at one measurement point on the rail for the first 6 hours of rail heating due to operation. The carriage moved back and forth at a constant velocity of 30 m/min. between the end points of an 800-mm stroke. Model adjustment, particularly quantification of the boundary conditions, such as moving friction and thermal conduction to the coupling structures, was conducted through experimental measurement values for heat build-up over the longer term. The temperature curves as a function of time (see Figure 7) confirmed that the model had accurately mapped the heat build-up on the rail. The final temperature obtained in the linear guide trail by FEM was 27.79 ˚C, whereas the temperature experimentally obtained was 27.20 ˚C with an error of 2.1%.

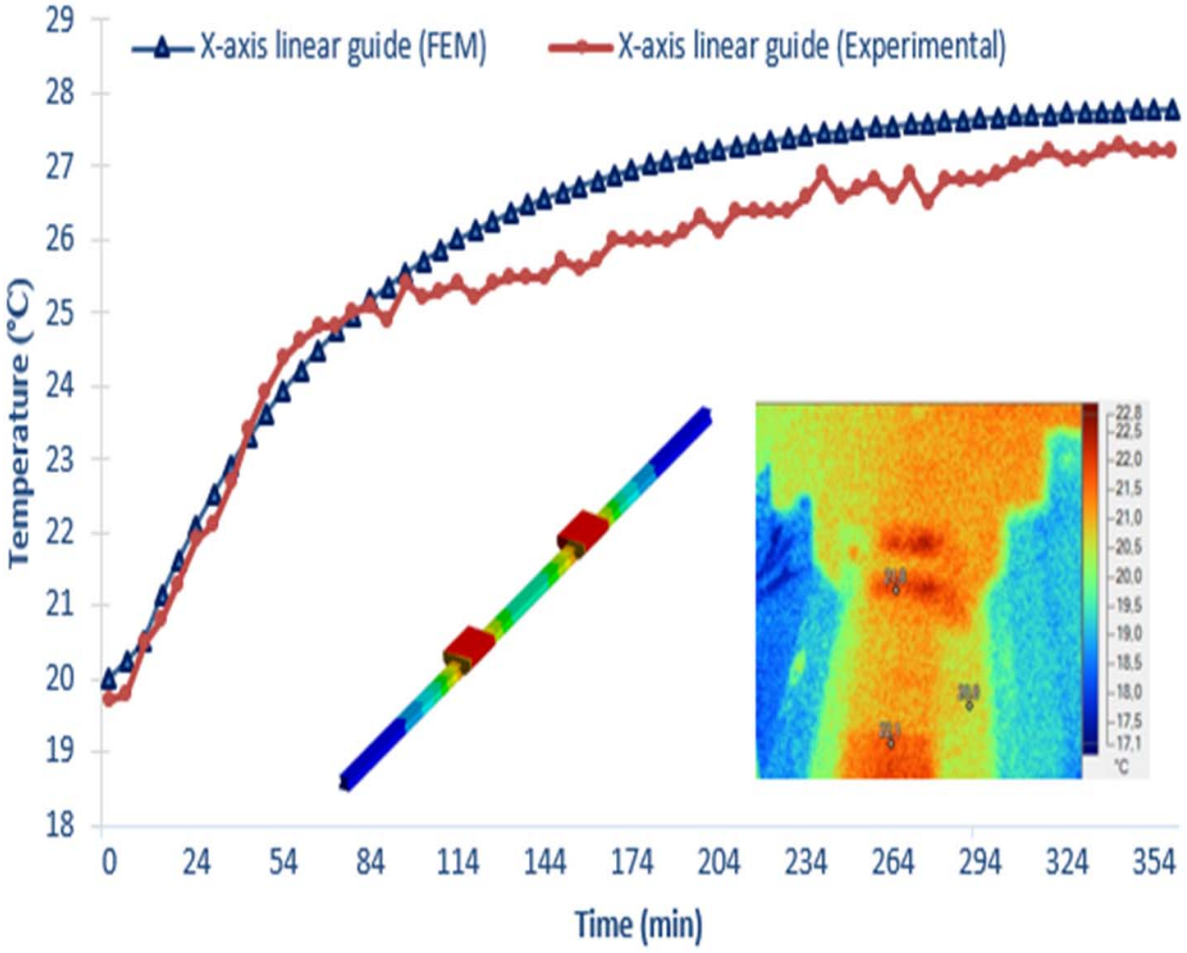

Figure 7. Comparison of the thermal behavior of the linear guide: experimental sensor reading T13 versus temperature predicted by FEM analysis.

Figure 8 graph illustrates the comparative evolution of the thermal behavior during the experimental measurements with the numerical analysis during a 6-hour operation with 30 m/min. speed. Note that the ball screw nut temperature rose as a function of time, and that the value obtained with the simulation precisely coincides with the value experimentally obtained (see Figure 8). This increase in temperature was due to the heat generated by the friction between the nut and the ball screw shaft contact in the round-trip displacement through an 800-mm course. The final temperature obtained in the linear guide trail by FEM was 35.30 ˚C, whereas the temperature experimentally obtained was of 34.70 ˚C, with an error of 1.7%.

Figure 9 shows the graph of the comparative evolution of the thermal behavior during the experimental measurements and the numerical analysis during a 6-hour operation with a 16,000-rpm speed. Note that the experimentally measured temperature increased quicker than the temperature obtained through the simulation. This is due to the need to adjust the forced convection thermal boundary condition at spindle tip. However, observe that both temperatures virtually reached the same final temperature. The final temperature obtained in the spindle tip region by FEM was 40.89 ˚C whereas the temperature obtained experimentally was 39.40 ˚C with a relative error of 3.8%. The largest errors occurred at the beginning of the analysis since the thermal stabilization in the simulation occurred more slowly. In the first thirty minutes, the maximum error reached 8.6%.

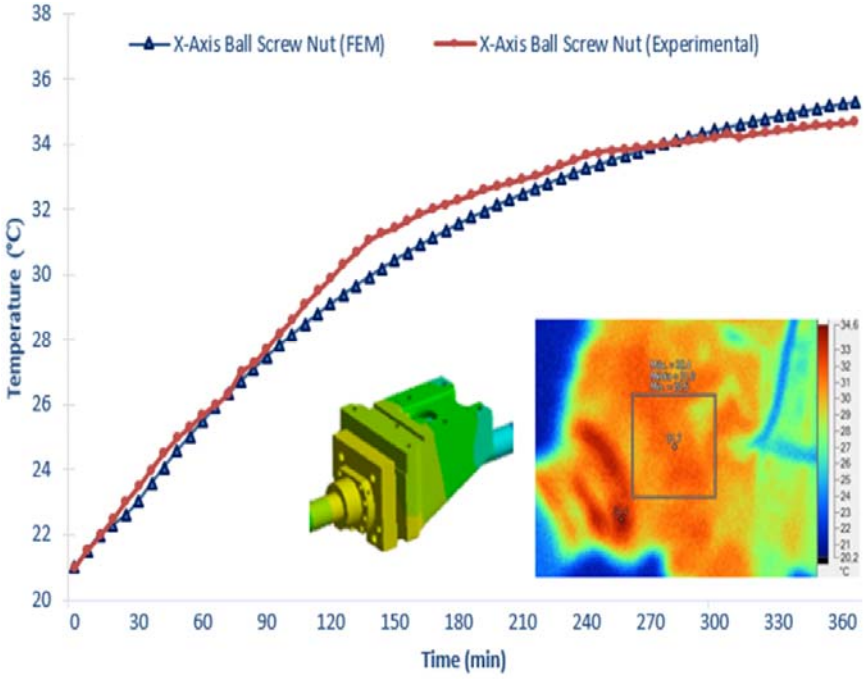

Figure 8. Comparison of the thermal behavior of the ball screw nut: experimental sensor reading T1 versus FEM temperatures predicted by simulation.

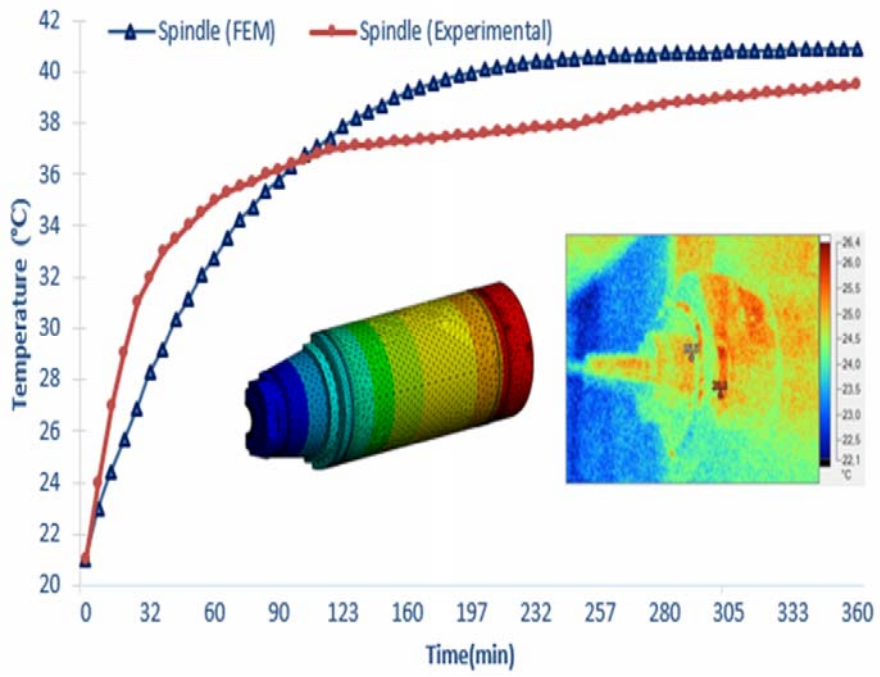

Figure 9. Comparison of the thermal behavior of the spindle: experimental sensor reading T10 versus temperature predicted by FEM analysis.

After validating the temperature fields for the X-axis ball screw, linear guide and spindle, the thermal boundary conditions, as well as the friction contacts modeled in the previous simulation, were reproduced in the transient thermal-structural analysis of the entire machining center for the third stage experimental cycle performed. In the FEM machine model, 409,786 second-order tetrahedral elements were used, totaling 737,629 nodes with element size of 50 mm in the machine structure, 40 mm in the worktable, and 25 mm in the slide units (see Figure 10). The ten-node tetrahedral elements of 10 mm were used around the contact surfaces to ensure more accurate results.

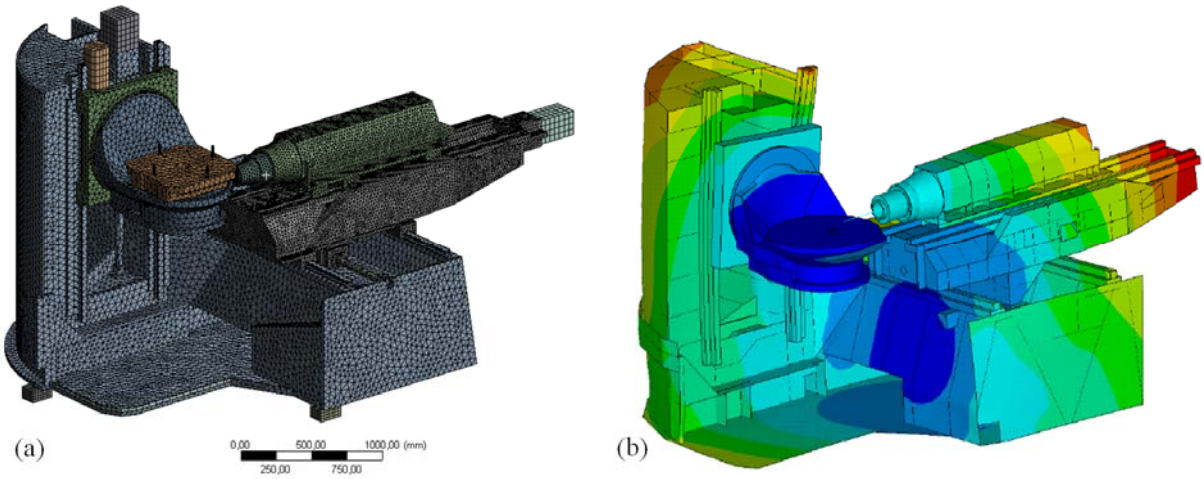

Figure 10. Machining center FEM analysis (a) finite element method mesh, (b) FEM predicted temperature field.

The temperature curves experimentally read by nine sensors are shown in Figure 11 in comparison with the results obtained by the FEM. The comparative results read by sensor T1 for the ball screw nut of the X-axis, sensor T3 for the linear guide of the X-axis and sensor T10 for the spindle have already been presented in the previous step, so they will not be represented in the graph of Figure 11.

Figure 11 allows verifying that, for all nine sensors represented, the same trend of temperature variation occurred in all cases. The maximum error for the T2 sensor located on the X-axis motor bearing was 2.7%, while the T11 and T12 sensors representing the temperatures read on the spindle housing and the machine base, respectively, did not exceed 3% error, either, between the simulated results and the experimental results. The error of the T7 sensor located on the Y-axis ball screw nut was 5.3% while the error of the T9 sensor located on the Y-axis motor bearing flange was 5.9%.

The T5 sensor located on the Z axis motor flange exhibited a maximum error of 9.6%, but the mean error was less than 6%. The T4 sensor located on the Z axis nut had a maximum error of 8.6% while the T6 sensor located on the Z axis linear guide showed a maximum error of 7.8%. The T14 sensors for the coolant tank and T15 sensor for the room temperature were not addressed since they did not present significant errors. The greatest errors occurred in the results obtained by the sensors located near the spindle, which can be explained by the difficulty in simulating all the heat generation due to the many spindle drives.

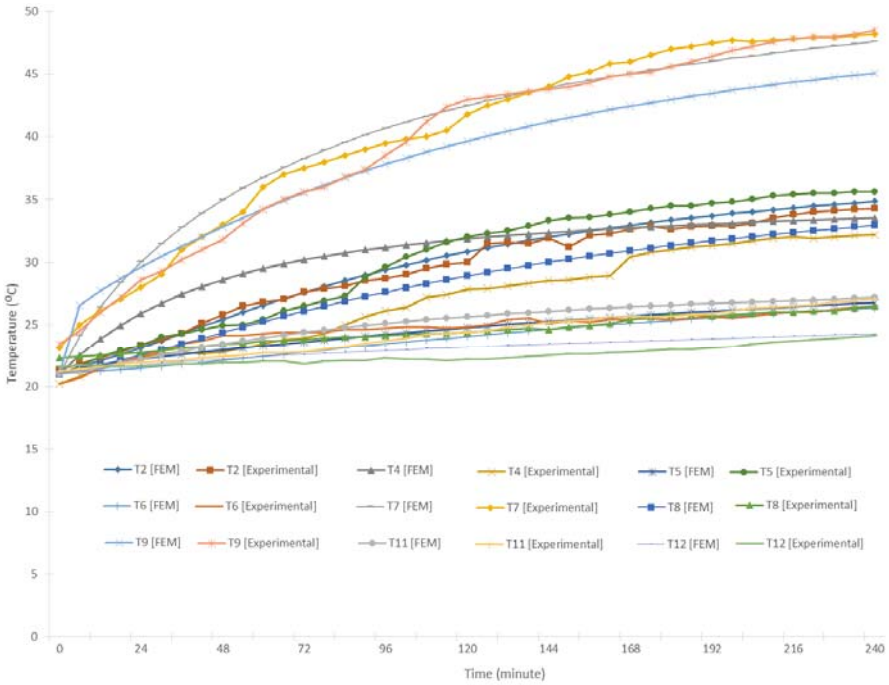

Figure 11. Temperature curves for all thermocouples measuring points during the third stage.

5. CONCLUSIONS

- This paper verified that thermal imaging and thermocouple temperature measurements, as well as thermal-structural simulation by the FEM and the methodology developed in this work, modeling frictional heat on the contact surface, provided significant results for estimating the thermal behavior of the main subsystems of a machining center, obtaining maximum errors of less than 10% and average errors around 6%.
- The conclusion is that the method, when appropriate boundary conditions are considered, is a proper feature for simulating the machine thermal behavior, which can still be used in the design phases of the equipment.
- After the thermal validation phase, the components of the thermal errors in the directions of the X, Y and Z axes could also be obtained through finite element analysis by measuring the displacement of the spindle in relation to the reference bush located in the machining table to estimate the thermal error of the machine.
- The methodology presented thus shows it can be used in actual cases of real-time thermal error compensation, proceeding to a later validation stage of the results numerically obtained in the machine tool.

6. ACKNOWLEDGEMENTS

The authors would like to acknowledge the companies B. GROB do Brazil and ESSS - ANSYS for their support in providing equipment and software.

7. REFERENCES

Feng, W., Li, Z., Gu, Q., Yang, J., 2015. “Thermally induced positioning error modelling and compensation based on thermal characteristic analysis”. International Journal of Machine Tools & Manufacture. 93, 26–36.

Großmann, K., Galant, A., Beitelschmidt, M., Partzsch, M., 2013. “Strukturveränderlichkeit in FEM und Blocksimulation bei der Berechnung von Temperaturfeldern”. 16. Dresdner Werkzeugmaschinen-Fachseminar – TU Dresden, IWM, Germany, pp 114 – 129.

Großmann, K., 2015. “Thermo-energetic Design of Machine Tools – A Systemic Approach to Solve the Conflict Between Power Efficiency, Accuracy and Productivity Demonstrated at the Example of Machining Production”. Ed. Springer Intern. Publ. pp 61 – 68. DOI: 10.1007/978-3-319-12625-8.

Lee, D.S., Choi, J.Y., Choi, D.H., 2003. “A based thermal source extraction and thermal distortion compensation method for a machine tool”. International Journal of Machine Tools & Manufacture, 43, 589–597.

Li, X., Xu, J., 2017. “Analysis of Fluid-Solid-Thermal Coupling for Ball Screw in Boring-Milling Machining Center”. 13th Global Congress on Manufacturing and Management, GCMM2016. Procedia Engineering. 174, 530 – 536.

Liu, H.; Miao, E.M.; Wei, X.Y. and Zhuang, X.D., 2017. “Robust modeling method for thermal error of CNC machine tools based on ridge regression algorithm”. International Journal of Machine Tools & Manufacture, 113, pp. 35-48. DOI: https://doi.org/10.1016/j.ijmachtools.2016.11.001

Ramesh, R., Mannan, M.A., Poo, A.N., 2000. “Error compensation in machine tools - a review Part II: thermal errors”. Int. J. Mach. Tools & Manuf. 40, 1257–1284.

Souza, R. F., 2013. “Desenvolvimento de uma metodologia para determinação e análise dos deslocamentos térmicos de máquinas-ferramenta usando o método dos elementos finitos e redes neurais artificiais”. 2013. 150p. Thesis (Doctor degree) – Universidade Federal da Paraíba. João Pessoa – PB, Brazil.

Wriggers, P., Miehe, C., 1994. “Contact constraints within coupled thermomechanical analysis – A finite element model”. Comput. Methods Appl. Mech. Eng. 113, 301-319.

Xu, M.; Jiang, S. and Cai, Y., 2007. “An improved thermal model for machine tool bearings”, International Journal Machine Tools & Manufacture, 47(1), pp. 53-62. DOI: https://doi.org/10.1016/j.ijmachtools.2006.02.018

Xu, Z.Z.; Liu, X.J.; Kim, H.K.; Shin, J.H. and Lyu, S.K., 2011. “Thermal error forecast and performance evaluation for an air-cooling ball screw system”, International Journal of Machine Tools & Manufacture, 51(7-8), pp. 605-11. DOI: https://doi.org/10.1016/j.ijmachtools.2011.04.001

Zhao, H., Yang, J., Shen, J., 2007. “Simulation of thermal behavior of a CNC machine tool spindle”, International Journal of Machine Tools & Manufacture, 47, (6), 1003–1010. https://doi.org/10.1016/j.ijmachtools.2006.06.018

Zwingenberger, C., Schädlich, K., Veselý, J., Neugebauer, R., 2008. “Simulation des Wärmegangs von Werkzeugmaschinen”. 80p. Fraunhofer Institut für Werkzeugmaschinen und Umformtechnik IWU, Germany.

8. RESPONSIBILITY NOTICE

The authors are the only responsible for the printed material included in this paper.